Removal of PM2.5 entering through the ventilation duct in an automobile using a carbon fiber ionizer-assisted cabin air filter

Jae Hong Park [a], Ki Young Yoon [b], Kwang Chul Noh [a], Jeong Hoon Byeon [c], Jungho Hwang [a,*]

[a] School of Mechanical Engineering, Yonsei University, Seoul 120-749, Republic of Korea
[b] Exhaust Emission Engineering Team, Hyundai Motor Company, Hwaseong 445-706, Republic of Korea
[c] LCD Division, Samsung Electronics Co., Ltd., Yongin 446-711, Republic of Korea

ARTICLE INFO

ABSTRACT

This study evaluated the charging characteristics of a carbon fiber ionizer for PM2.5 and carried out particle capture laboratory tests after an ionizer was installed upstream of the media of an electret cabin air filter. When the ion concentration per particle (N_i) of the carbon fiber charger was 10^6 ions/cm^3, the average charge numbers for each particle were 1.54, 0.88, and 0.49 at 0.6, 1.2, and 1.8 m/s of face velocity, respectively (the particle charging times, τ, were 167, 83, and 56 ms, respectively). For these face velocities, the PM2.5 removal efficiencies of the filter media were 69.3%, 65.2% and 62.2%, respectively, but increased to 80.4%, 71.2% and 65.5%, respectively, when the ionizer was turned on. The carbon fiber ionizer was then installed in front of an electret cabin filter in the air conditioning system of an automobile, after which field tests were performed at a roadside area. For the same $N_i\tau$ used in the lab-scale tests, the effects of the carbon fiber ionizer on increasing PM2.5 %Reduction were mild as 9.4%, 4.0%, and 2.8% when the flow rates were at the second, fourth, and sixth levels, respectively (the face velocities were 0.6, 1.2, and 1.8 m/s, respectively). The PM2.5 %Reduction can be substantially increased by 20–21%, for a higher value of $N_i\tau$ ($=1.0 \times 10^8$ ions s/cm^3), which is realized by increasing the power consumption of the carbon fiber ionizer.

1. Introduction

Automobile cabin exposure to pollutants is high because of the proximity of the passengers to relatively undiluted emissions from other automobiles and the rapid air exchange rate inside vehicles (Park et al., 1998). Moreover, roadway conditions, such as traffic congestion, appear to contribute to onboard pollution levels, as does the intrusion into the cabin of pollution produced by one's own vehicle (Adar et al., 2008; Sabin et al., 2005). The automobile cabin air filter, which is a type of electret filter, has been used to capture particles penetrating into automobile passenger compartments through the ventilation duct. Electret filters are deep-bed fibrous filters used in air filtration that are composed of highly porous, coarse fibers, which allow for only a low flow resistance. Since the fibers are permanently charged, electrical forces act between the fibers and any particles present (Emi, Kanaoka, Otani, & Ishiguro, 1987).

The particle capture capabilities of electret filters rely on a combination of conventional mechanical mechanisms (i.e. impaction, interception, and diffusion) and electrostatic mechanisms. If the particles are charged, an enhanced Coulombic force will affect particle capture. Numerous studies have been carried out to understand the effects of particle charging on

---

* Corresponding author. Tel.: +82 2 2123 2821; fax: +82 2 312 2821.
  E-mail address: hwangjh@yonsei.ac.kr (J. Hwang).

increasing the efficiency of electret filters. Kim, Otani, Noto, Namiki, and Kimura (2005) studied the initial collection performance of uncharged and single-charged particles using resin wool electret filters. Fjeld and Owens (1988) and Kanaoka, Emi, Otani, and Iiyama (1987) investigated the effect of particle charges on penetration. Since the efficiency of an electret filter depends on the charge state, particles with higher charges are more easily removed than particles with a natural charge. One example of a traditional particle charging system is that of corona discharge (Qi, Chen, & Pui, 2007; Unger, Boulaud, & Borra, 2004). To investigate this system, Lee et al. (2001) carried out an experimental study involving electret filters coupled with a corona pre-charger.

Recently, Han, Kim, Kim, and Sioutas (2008) examined a carbon brush-type ionizer with an ion emission tip consisting of a bundle of micron-sized carbon fibers. Each fiber was supplied with a high voltage, and ions were emitted from the ends of the fiber. The carbon fiber ionizer produced stable unipolar ions in sufficiently high concentrations without generating particulate matter or ozone. Park, Yoon, Kim, Byeon, and Hwang (2009) examined the effect of a carbon fiber ionizer on particle charging and capture on the media of a fibrous medium filter. Submicron-sized aerosol particles were selected because of their relatively low charging capabilities and collection efficiencies in comparison to those of micro-sized aerosol particles.

This study evaluated the charging characteristics of the ionizer used in Park et al. (2009) for PM2.5 and carried out lab tests on particle capture after the ionizer was installed upstream of electret cabin air filter media. The carbon fiber ionizer was then installed in front of the electret cabin filter in the air conditioning system of an automobile, after which field tests were performed. In order to simulate the relationship between PM2.5 concentrations of in-automobile and outdoor air, the mass-balance particle dynamic equation was utilized. Parameters based on the results of lab-scale tests, such as ventilation, deposition, and filtration, were determined. The calculated results were then compared with actual field measurements.

2. Experimental

Lab-scale tests were performed with the experimental setup shown in Fig. 1. The lab-scale test system consisted of a test duct, a particle generation system, and a measurement system. The test duct, with a cross-sectional area of $0.04 \times 0.04 \ m^2$ and a length of 1 m, consisted of acryl. A cabin air filter composed of electret fibers was installed in the middle of the test duct. Table 1 lists the specifications of the cabin air filter used in this study. Two isokinetic sampling probes, made of stainless steel, were located at the front and back of the filter media for aerosol sampling.

Used as test particles, a steady-state concentration of potassium chloride (KCl) particles was supplied to the test duct. The test particles were generated according to the ANSI/ASHRAE standard (ASHRAE, 2007). A branch of particle-free, compressed air from a dry-clean air supply system consisting of an oil trap, a diffusion dryer, and a high-efficiency particulate air (HEPA) filter was delivered to a Collison-type atomizer with a solution containing aqueous KCl 30% by
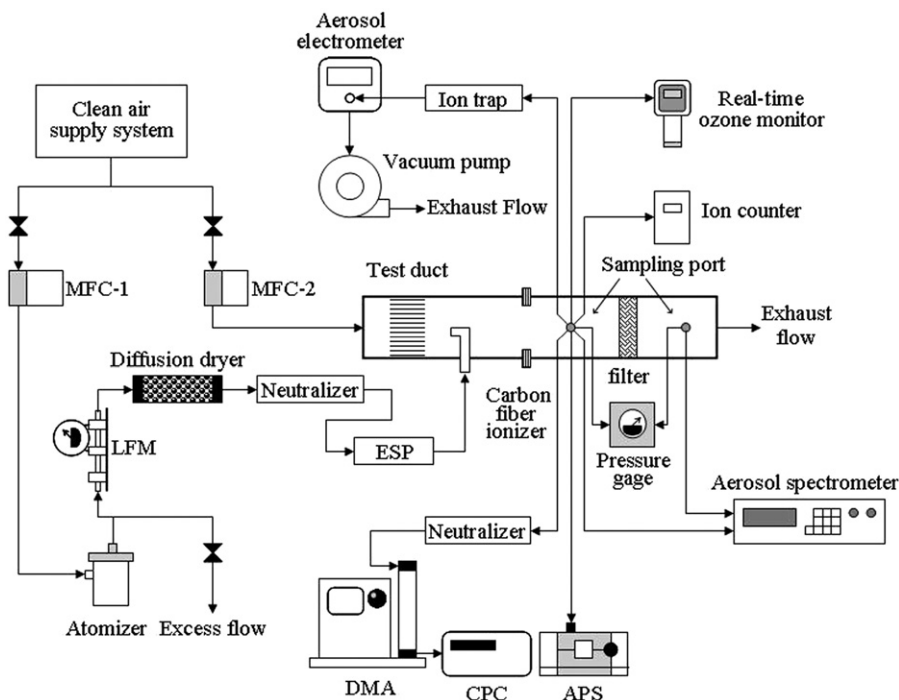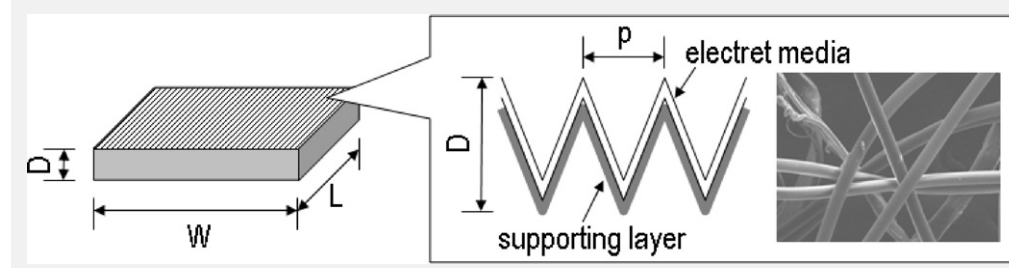

Fig. 1. Experimental setup (lab-scale test).

Table 1
Specifications of the cabin air filter.

Size (mm)		p (mm)	Media material	Fiber diameter (μm)	Solidity
Lab. test	Field test				
$W=40$ $L=40$ $D=17$	$W=225$ $L=202$ $D=17$	6	Electret polypropylene × supporting layer: polyester	10	0.009–0.010

weight to generate test particles for the PM2.5. The test particles from the atomizer passed through a diffusion dryer for water removal and then a neutralizer (Soft X-ray charger 4530, HCT Co., Ltd., Icheon-si, Gyeonggi-do, Korea) for charge neutralization. The test particles from the neutralizer then passed through an electrostatic precipitator (ESP), where an average electric field of 5 kV/cm was used to remove the charged particles and deliver the uncharged particles to the test duct. Use of a laminar flow meter (LFM) helped control the desired concentrations of test particles controlled. Another portion of clean air was delivered to the test duct and mixed with the particle-laden air flow. The mixture flow rates varied from 57.6 to 115.2 to 172.8 l/min in order to achieve velocities of 0.6, 1.2, and 1.8 m/s at the filter media, respectively. A pair of carbon fiber ionizers were positioned at both the top and bottom of the test duct, 10 cm ahead of the filter media. Each carbon fiber ionizer consisted of an ion emission tip and a power pack. The ion emission tip consisted of a 300 ± 50 carbon fiber bundle and the diameter of each carbon fiber was approximately 5–10 μm. The input voltage of the power pack was 220 V (AC, 60 Hz), and the maximum output voltage of the power pack was a 4-kV (peak-to-peak, 60 Hz) saw-tooth wave form with an operation current of less than a few μA. A rheostat controlled the operation voltage, and thus the total power consumption was less than 1 W. The rheostat controlled the ion generation concentration, which was maintained at 6.0×10^9 ions/cm^3.

An ion counter measured gaseous ion concentrations (Air ion counter, AlphaLab, Inc., Salt Lake City, UT, USA). An aerodynamic particle sizer (APS, 3321, TSI, Shoreview, MN, USA) and a scanning mobility particle sizer (SMPS, 3936L22, TSI, Shoreview, MN, USA) measured the total masses and number concentrations of the test particles, depending on their size ranges. The SMPS consisted of a classifier controller (3080, TSI, Shoreview, MN, USA), differential mobility analyzer (DMA, 3081, TSI, Shoreview, MN, USA), condensation particle counter (CPC, 3022 A, TSI, Shoreview, MN, USA), and aerosol charge neutralizer (Soft X-ray charger 4530, HCT Co., Ltd., Icheon-si, Korea) with a sampling air flow rate of 0.3 l/min. The SMPS measures particles from 0.0025 to 1.0 μm with a mobility equivalent diameter. The APS measures particles from 0.5 to 20 μm with an aerodynamic diameter and a sampling air flow rate of 5 l/min by using a double-crest optical system. The total mass concentrations of the test particles were also measured with an aerosol spectrometer (model 1.109, Grimm, Ainring, Germany) at a sampling air flow rate of 1.2 l/min. The aerosol spectrometer was the measurement device used to determine the number concentration and mass fractions of the aerosols. It can detect airborne aerosol particles from 0.25 to 32 μm of optical equivalent diameter by using a form of light scattering detection. The average charge per particle was estimated with a current measurement using an aerosol electrometer (3068A, TSI, Shoreview, MN, USA), and the air was sampled at an air flow rate of 5 l/min using a vacuum pump. The sampled air flow passed through an ion trap, where an average electric field of 150 V/cm was applied to eliminate gaseous ions. The average charge per particle ($n_{C,Avg}$) was then calculated using the following equation:

$$n_{C,Avg} = \frac{I}{NQe} \tag{1}$$

where N is the total number concentration of test particles, obtained from the SMPS and APS measurements. I is the current, Q is the sampling flow rate, and e is the elementary unit of charge ($=1.6 \times 10^{-19}$ coulomb). A pressure gauge was used to measure the pressure drop across the filter media. The ozone concentration, measured with an O$_3$ monitor (PortaSensII, Ati, Collegeville, PA, USA), was below the detection limit of 0.01 ppm when the carbon fiber ionizers were turned on. The temperature and relative humidity inside the test duct were 22.5 ± 3 °C and 10 ± 5%, respectively.

Field tests were carried out at a roadside area. A test car (New Pride, 1.5 l diesel engine, Kia Motors Corp., Seoul, Korea) was left running in idle mode, and the volume of automobile cabin air was 2.5 m^3. The schematic for the field test is shown in Fig. 2.
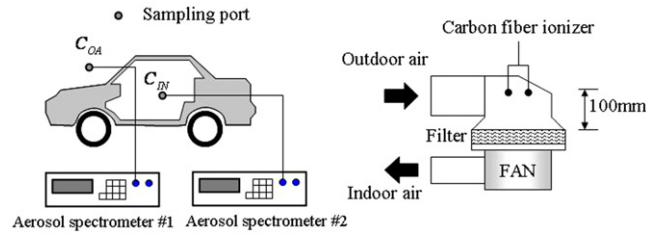
Fig. 2. Experimental setup (field test).

Table 2
Operation conditions for cabin flow.

Operation mode	Flow level	Face velocity at cabin air filter (m/s)	Total flow rate (m³/h)
	2	0.6	97
	4	1.4	195
	6	1.8	292

Two carbon fiber ionizers were installed 10 cm in front of the cabin air filter of the air conditioning system. A fan controlled the flow rate, as shown in Table 2, at levels of two, four, and six, resulting in face velocities of 0.6, 1.2, and 1.8 m/s, respectively. The total mass concentrations of PM2.5 of the outdoor air and in-automobile air were measured with two aerosol spectrometers (model 1.109, Grimm, Ainring, Germany). The outdoor particle concentration of PM2.5 was approximately 100 ± 10 μg/m³. The atmospheric temperature and relative humidity were 27 ± 3 °C and 50 ± 5%, respectively.

3. Results and discussion

3.1. Lab-scale tests of PM2.5 removal

Fig. 3 shows the pressure drops across the cabin air filter media for various face velocities. The data were compared with theoretical predictions calculated from the following equation (Langmuir, 1942):

$$\Delta p = \frac{2C_D \alpha \rho U^2 L}{\pi g d_f (1-\alpha)} \tag{2}$$

where C_D is the drag coefficient, α is the filter solidity, ρ is the air density, U is the face velocity, L is the depth of the filter, g is the gravitational acceleration, and d_f is the fiber diameter of filter. C_D is defined as

$$C_D = \frac{11.2\pi}{Re(-\ln \alpha + 2\alpha - (\alpha^2/2) - (3/2))} \tag{3}$$

where Re is the Reynolds number. The calculations agreed well with the data for $\alpha = 0.0009$–0.001, as shown in Table 1.

The size distribution of the test particles was measured by APS and SMPS. The results are shown in Fig. 4. The mobility was converted to an aerodynamic diameter on the basis of the equation below

$$d_A = d_M \left(\frac{\rho_P C_C(d_M)}{\chi \rho_0 C_C(d_A)} \right)^{0.5} \tag{4}$$

where d_A is the aerodynamic diameter measured by the APS, d_M the mobility equivalent diameter measured by the SMPS, C_C is the Cunningham correction factor, χ is the dynamic shape factor ($=1$ for a spherical particle), ρ_P is the KCl particle density ($=1.987$ g/cm³), and ρ_0 is the unit density ($=1$ g/cm³). From Fig. 4, the total mass concentration and total number concentration were 100 ± 5 μg/m³ and 5850 ± 50 particles/cm³, respectively. The total mass concentration of test particles was measured by aerosol spectrometer ($=100$ μg/m³) and agreed well with the concentration obtained from the APS and SMPS measurements.
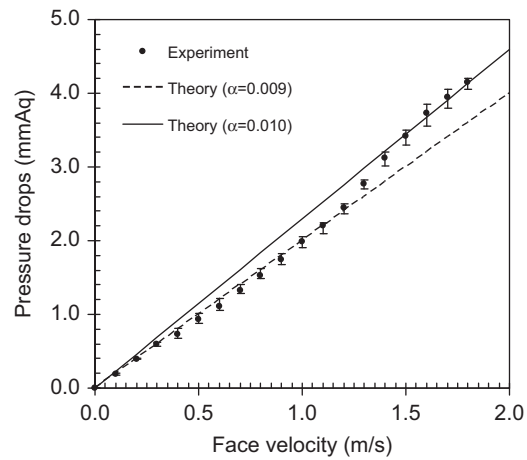
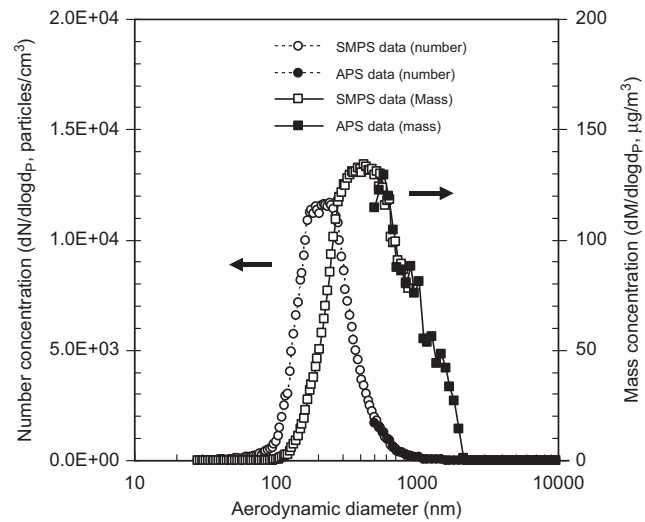**Fig. 3.** Pressure drop vs. face velocity.

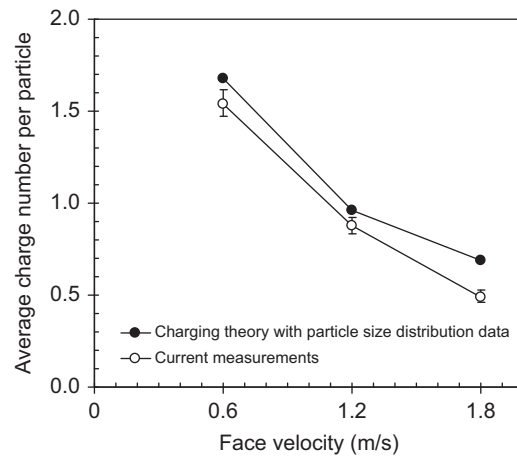**Fig. 4.** Size distribution of the test particles.

Fig. 5. Average charge number per particle according to face velocity.

The average charge number per particle was calculated, and the results are shown in Fig. 5. By considering only the diffusional charging mechanism, the theoretical charge number per particle, n_C, is defined as follows (Hinds, 1999):

$$n_C(d_A) = \frac{d_A kT}{2K_E e^2} \ln\left[1 + \frac{\pi K_E d_A c_i e^2 N_i \tau}{2kT}\right] \tag{5}$$

where K_E is the electrostatic constant of proportionality ($=9 \times 10^9$ N m^2/C^2), T is the charging time, c_i is the mean thermal speed of air ions ($=2.4 \times 10^2$ m/s), k is the Boltzmann constant ($=1.381 \times 10^{-23}$ J/K) and T is the temperature and N_i is the concentration of ions per particle. N_i was calculated by the following equation:

$$N_i = \frac{N_{ion}}{NV_0} \tag{6}$$

where N_{ion} is the ion concentration generated by carbon fiber ionizer ($=6.0 \times 10^9$ ions/cm^3) and V_0 is the unit volume ($=1$ cm^3). The average charge number per particle was calculated by the following equation:

$$n_{C,Avg} = \frac{\sum n_C(d_A) n(d_A)}{\sum n(d_A)} \tag{7}$$

where $n(d_A)$ is the particle number concentration at size d_A, obtained from the SMPS and APS measurements. The average charge numbers per particle were calculated to be 1.68, 0.96, and 0.69, at 0.6, 1.2, and 1.8 m/s of face velocity, respectively. These calculated results agreed well with the experimental results of 1.54, 0.88, and 0.49, at 0.6, 1.2, and 1.8 m/s of face velocity, respectively.

Fig. 6 shows the effect of air ionization on the PM2.5 removal efficiency of the filter media with and without the carbon fiber ionizers. The PM2.5 removal efficiency is defined as

$$\eta_{PM2.5} = 1 - \frac{C_{downstream}}{C_{upstream}} \tag{8}$$

where C is the total mass concentration of PM2.5 ($C_{upstream} = 100 \pm 5$ μg/m^3). As the face velocity increased, the PM2.5 removal efficiency decreased, regardless of the operation of the carbon fiber ionizers. Moreover, as Fig. 6 shows, the particle removal efficiency increased with the use of ionizers. The change in PM2.5 removal efficiency with the use of carbon fiber ionizers was 11.1% at a face velocity of 0.6 m/s but decreased to 6.0% and 3.4% at 1.2 and 1.8 m/s, respectively. Particle wall losses with the use of a carbon fiber ionizer were below 4%.

Fig. 6 shows the theoretical results of particle removal efficiency defined by the following equation:

$$\eta_{PM2.5} = \frac{\sum \eta(d_A) d_A^3 n(d_A)}{\sum d_A^3 n(d_A)} \tag{9}$$

The particle removal efficiency $\eta(d_A)$ is defined as (Hinds, 1999)

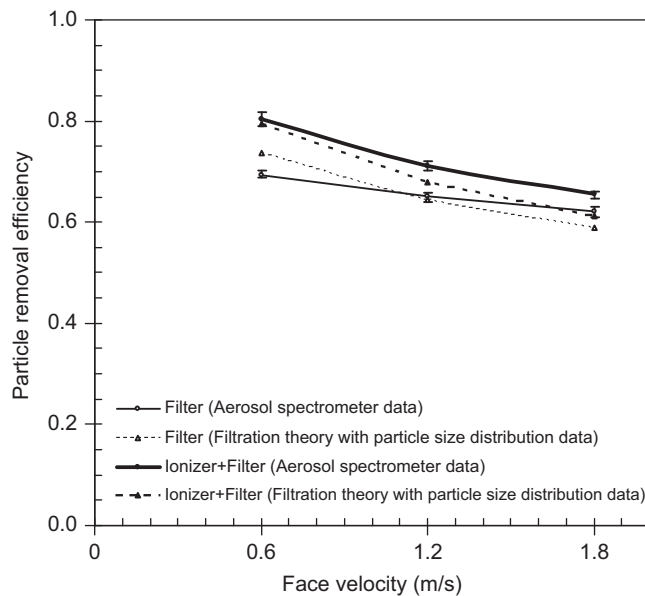$$\eta(d_A) = 1 - \exp\left[-\frac{4\alpha \ell E(d_A)}{\pi d_f (1-\alpha)}\right] \tag{10}$$

Fig. 6. Particle removal efficiency of PM2.5 according to face velocity.

where ℓ is the filter depth and $E(d_A)$ is the single-fiber efficiency. For uncharged particles, $E(d_A)$ contains two dimensionless parameters appropriate for capture by diffusion and polarization forces and can be expressed as (Brown, 1993; Kanaoka et al., 1987)

$$E(d_A) = 1.07 Pe^{-2/3} + 0.06 N_{p0}^{2/5} \tag{11}$$

where Pe is the Peclet number ($= d_f u_0 / D$), and D is the diffusion coefficient depending on the particle size d_A. u_0 is the face velocity at the fiber of the filter ($= U/(1-\alpha)$). The polarization force parameter N_{p0} is defined by the ratio of the polarization force between the charged fiber and the uncharged particle to air drag as

$$N_{p0} = \frac{2}{3} \times \frac{\varepsilon_p - 1}{\varepsilon_p + 2} \times \frac{\sigma^2 d_A^2 C_C}{\varepsilon_0 (1 + \varepsilon_f)^2 d_f \mu u_0} \tag{12}$$

where ε_p is the dielectric constant of the test particle (KCl=4.6), ε_f is the dielectric constant of the filter fiber (polypropylene=2.2), σ is the surface charge density on the fiber ($= 3.2 \times 10^{-4}$ C/m^2), ε_0 is the permittivity ($= 8.855 \times 10^{-12}$ F/m), and μ is the air viscosity ($= 1.81 \times 10^{-5}$ kg/m s).

For charged particles, not only the diffusion and polarization forces but also the Coulombic force are effective for removing particles. Hence, to evaluate the effect of the Coulombic force, $E(d_A)$ can be expressed as (Brown, 1993)

$$E(d_A) = 1.07 Pe^{-2/3} + 0.06 N_{p0}^{2/5} + 0.067 N_{pq}^{3/4} - 0.017 (N_{p0} N_{pq})^{1/2} \tag{13}$$

where the Coulombic force parameter N_{pq}, defined as

$$N_{pq} = \frac{n_C(d_A) e \sigma C_C}{3 \pi \mu \varepsilon_0 (1 + \varepsilon_f) d_A u_0} \tag{14}$$

Since the average charge number particle decreased with an increase in the flow rate (in Fig. 5), the decrease of the Coulombic force parameter resulted in a decrease of single-fiber efficiency (in Eq. (13)). The calculation results based on the filtration theory agree well with the aerosol spectrometer data shown in Fig. 6.

3.2. Field tests of PM2.5 removal

The effect of the carbon fiber ionizer-assisted cabin air filter on particle removal can be evaluated with the following equation:

$$\%\text{Reduction} = \left(1 - \frac{C_{IN}}{C_{OA}}\right) \times 100 \tag{15}$$

where C_{IN} is the total mass concentration of PM2.5 in indoor air, and C_{OA} is the total mass concentration of PM2.5 in outdoor air ($= 100 \pm 10$ μg/m^3). For the schematic shown in Fig. 7, the indoor particle concentration, C_{IN}, can be calculated from the following mass balance equation:

$$V \frac{dC_{IN}}{dt} = C_{OA}(\dot{Q}_S (1 - \eta_{PM2.5})) - C_{IN}(\dot{Q}_S + \dot{\beta}) + \dot{S} \tag{16}$$

where V is the cabin volume, t is the operation time, $\dot{Q}_S$ is the air flow rate supplied into the cabin, $\dot{S}$ is the generation rate of PM2.5, and $\dot{\beta}$ is the deposition rate of particles onto the in-automobile wall, which is defined as

$$\dot{\beta} = V_{dep} A_{dep} \tag{17}$$

where V_{dep} is the deposition velocity of PM2.5 and A_{dep} is the deposition area. V_{dep} was assumed to be at 0.5×10^{-4} m/s (Hinds, 1999; Schneider & Bohgard, 2005), and A_{dep} was approximately 12.5 m^2. $\dot{S}$ was assumed to be zero. The steady-state solution of Eq. (16) becomes

$$C_{IN} = \frac{C_{OA} \dot{Q}_S (1 - \eta_{PM2.5})}{\dot{Q}_S + \dot{\beta}} \tag{18}$$
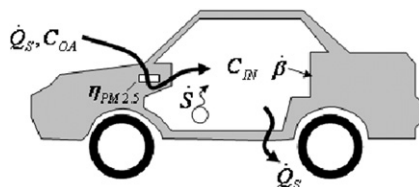

Fig. 7. Schematic of a mass balance model.

The forced flow rate to the cabin through the ventilation duct was controlled. Table 2 summarizes the three operation conditions of the cabin flow. Fig. 8 shows the experimental data and calculated results for various %Reductions. Overall, the calculated results well predicted the experimental results. When the flow level increased, the in-automobile ventilation rate increased and the %Reductions decreased, regardless of whether the ionizer was used. When the operation mode was at the second level of flow, the steady-state values of %Reduction with and without ionizers were 68.3% and 77.7%, respectively. When the flow level increased, the effect of the ionizer decreased. This relation was due to a decrease in the removal efficiency for the PM2.5 because of the decrease in particle charging time. The attachment of gaseous ions onto the particles may increase the Coulombic forces between the particles and the filter fibers. When the flow rate increased, the time required for particle charging decreased, resulting in decreased particle charge, which can be expressed as shown in Eq. (5).

3.3. Application of ionizer to practical purposes

So far the experimental results of lab-scale tests and field tests were presented and discussed when the carbon fiber charger was operated such that the range of $N_i\tau$ was 5.7×10^4–17×10^4ions s/cm^3. Supplementary experiments and calculations were carried out to show that the carbon fiber charger can make a substantial difference on the removal efficiency, if a higher value of $N_i\tau$ is utilized. Fig. 9 shows that when the ionizer is not used, $\eta_{PM2.5}$ are 73.6%, 64.4% and 58.9%, respectively, for face velocities of 0.6, 1.2, and 1.8 m/s, but increase to 94.0%, 85.7% and 79.2%, respectively, when the
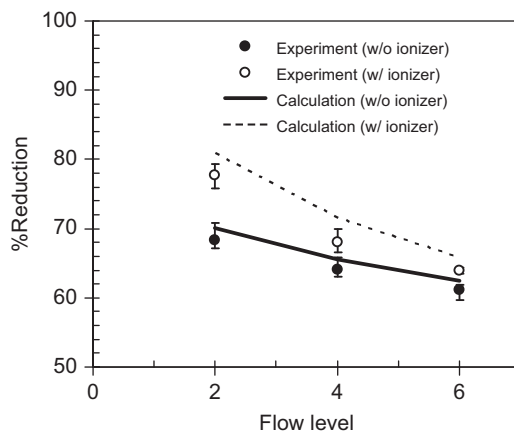

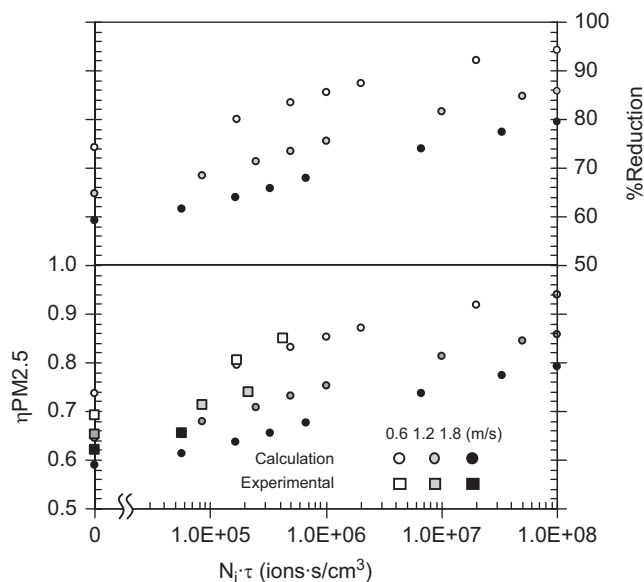**Fig. 8.** Percentage reductions with operation flow.

Fig. 9. Particle removal efficiency and %Reduction with variation of the product of charging time and ion concentration per particle.

ionizer is operated for $N_i\tau$ of 1.0×10^8 ions s/cm^3. The corresponding effects of the carbon fiber ionizer on increasing PM2.5 %Reduction in the field tests will be 20–21% for face velocities of 0.6–1.8 m/s. For practical applications, obtaining this high value of $N_i\tau$ may not be easy by increasing the charging time with increasing the length of the charging section, owing to the limited space of the duct where the cabin filter is inserted. However, this high value of $N_i\tau$ can be easily realized by increasing the power consumption with decreasing the rheostat of the power pack.

4. Conclusions

We evaluated the charging characteristics of a carbon fiber ionizer for PM2.5 and carried out lab tests for particle capture after an ionizer was installed upstream of an electret cabin air filter media. When the ion concentration per particle of the carbon fiber charger was 10^6 ions/cm^3, the average charge numbers for each particle were 1.54, 0.88, and 0.49 at 0.6, 1.2, and 1.8 m/s of face velocity, respectively (the particle charging times were 167, 83, and 56 ms, respectively). For these face velocities, the PM2.5 removal efficiencies of the filter media were 69.3%, 65.2% and 62.2%, respectively, and increased to 80.4%, 71.2% and 65.5%, respectively, when the ionizer was used. When the flow rate increased, the time required for particle charging decreased, resulting in an overall decrease of particle charge. The carbon fiber ionizer was then installed in front of an electret cabin filter in the air conditioning system of an automobile, and field tests were performed at a roadside area. To simulate the relationship between PM2.5 concentrations of in-automobile air and outdoor air, the mass-balance particle dynamic equation was used. The calculated results were then compared with field measurements. For the same $N_i\tau$ used in the lab-scale tests, the effects of the carbon fiber ionizer on increasing PM2.5 %Reduction were mild as 9.4%, 4.0%, and 2.8% when the flow rates were at the second, fourth, and sixth levels, respectively. The PM2.5%Reduction can be substantially increased by 20–21%, for a higher value of $N_i\tau$ (1.0×10^8 ions s/cm^3), which is realized by increasing the power consumption of the carbon fiber ionizer.

References

Adar, S. D., Davey, M., Sullivan, J. R., Compher, M., Szpiro, A., & Liu, L.-J. S. (2008). Predicting airborne particle levels aboard Washington State school buses. *Atmospheric Environment*, *42*, 7590–7599.

ASHRAE, L.-J. S. (2007). *Method of Testing General Ventilation Air-cleaning Devices for Removal Efficiency by Particle Size*. Atlanta, GA: American Society of Heating, Refrigerating and Air-Conditioning, Engineers, Inc. [ANSI/ASHRAE standard 522-2007].

Brown, R. C. (1993). *Aerosol Filtration: An Integrated Approach to the Theory and Applications of Fibrous Filters*. Oxford: Pergamon Press.

Emi, H., Kanaoka, C., Otani, Y., & Ishiguro., T. (1987). Collection mechanisms of electret filter. *Particulate Science and Technology*, *5*, 161–171.

Fjeld, R. A., & Owens, T. M. (1988). The effect of particle charge on penetration in an electret filter. *IEEE Transactions on Industrial Applications*, *24*, 725–731.

Han, B., Kim, H. J., Kim, Y. J., & Sioutas, C. (2008). Unipolar charging of fine and ultra-fine particles using carbon fiber ionizers. *Aerosol Science and Technology*, *42*, 793–800.

Hinds, W. C. (1999). *Aerosol Technology: Properties, Behavior, and Measurement of Airborne Particles* ((2nd ed.). New York: John Wiley & Sons, Inc.

Kanaoka, C., Emi, H., Otani, Y., & Iiyama, T. (1987). Effect of charging state of particles on electret filtration. *Aerosol Science and Technology*, *7*, 1–13.

Kim, J. C., Otani, Y., Noto, D., Namiki, N., & Kimura, K. (2005). Initial collection performance of resin wool filters and estimation of charge density. *Aerosol Science and Technology*, *39*, 501–508.

Langmuir, I., 1942. Report of smokes and filters. Part IV of a reports for the office of scientific research and development, OSRD, no. 865, ser. no. 353 Rodebush et al. 1942 Filtration of aerosols and development of filter materials. Technical Report.

Lee, J. K., Kim, S. C., Shin, J. H., Lee, J. E., Ku, J. H., & Shin, H. S. (2001). Performance evaluation of electrostatically augmented air filters coupled with a corona precharger. *Aerosol Science and Technology*, *35*, 785–791.

Park, J. H., Spengler, J. D., Yoon, D. W., Dumyahn, T., Lee, K., & Ozkaynak, H. (1998). Measurement of air exchange rate of stationary vehicles and estimation of in-vehicle exposure. *Journal of Exposure Science and Environmental Epidemiology*, *8*, 65–78.

Park, J. H., Yoon, K. Y., Kim, Y. S., Byeon, J. H., & Hwang, J. (2009). Removal of submicron aerosol particles and bioaerosols using carbon fiber ionizer assisted fibrous medium filter media. *Journal of Mechanical Science and Technology*, *23*, 1846–1851.

Qi, C., Chen, D. R., & Pui, D. Y.H. (2007). Experimental study of a new corona-based unipolar aerosol charger. *Journal of Aerosol Science*, *38*, 775–792.

Sabin, L. D., Behrentz, E., Winer, A. M., Jeong, S., Fitz, D. R. Pankratz, D. V., et al. (2005). Characterizing the range of children's air pollutant exposure during school bus commutes. *Journal of Exposure Analysis and Environmental Epidemiology*, *15*, 377–387.

Schneider, T., & Bohgard, M. (2005). Airborne particle deposition onto the ocular surface. *Indoor Air*, *15*, 215–219.

Unger, L., Boulaud, D., & Borra, J. P. (2004). Unipolar field charging of particles by electrical discharge: effect of particle shape. *Journal of Aerosol Science*, *35*, 965–979.